COMPUTER SYSTEM FOR MULTISPECTRAL IMAGE ACQUASITION AND PROCESSING

B. Wiecek, Z. Zwolenik, R. Danych
Institute of Electronics, Technical University of Lodz, Poland

Abstract- **In this paper, multi-input computer system for image acquisition and processing is presented. This system is equipped with 2-wavelength thermal channel and any 4 other one, which can be used to capture visual, X-ray, ultrasound images, etc. Novel image processing tools are described, mainly for geometrical and 3D transformations.**

Keywords – **Image processing, thermography, 3D scene reconstruction, geometry correction, emissivity.**

I. INTRODUCTION

The system contains analog and digital part as shown in *Fig. 1*. In the analog block, two 16-bit A/D converters are used to convert thermal and visual images. CCD flash ADC is equipped with 4-input analog multiplexer. It makes possible to capture visual images one-by-one, with the delay of one frame (20ms), but in parallel with thermal image. In the digital part 1-2MB buffer VRAM memory is used to store images and transfer them to the computer. A dual-port memory is suitable for fast data acquisition, and it allows to synchronize easy the data capturing and transferring into the operational memory. Entire control system is integrated in high density FPGA (Field Programmable Gate Array), providing high flexibility of the design and possibility of system reconfiguration for different cameras. Actually, our system is prepared for thermal cameras with both the analog and the digital outputs.

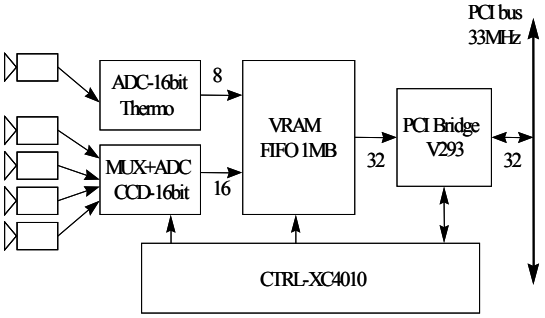

Fig. 1. System block diagram

Sampling clock restoration is one of the most important circuit. Sampling rate of video signal (CCIRT-PAL) at 14.75MHz ensures the square pixel and the proper image size on the screen. Video capturing circuit works with clock restoration using the Digital Phase Lock Loop circuitry (DPLL). This causes the high stability of the restored sampling clock and in consequence the high quality of the captured image. DPLL-based restoration circuit is recommended in high-resolution video systems, where the slight changes in the phase clock can disturb the captured image smoothness [3-4]. The memory buffer implemented as fast dual-port memories (VRAM) is designed as a FIFO (First-In-First-Out) memory. Input data coming from A/D converters is loaded into the memory through Serial Register (SAM). The corresponding line counter for locating the memory row, where the pixels are placed in, is implemented in FPGA. This control block contains also similar counters for pixels and lines to read data from the memory and transfer them to the computer. The main parameters of multichannel system are presented in *Table I*.

TABLE I
BASIC SYSTEM PARAMETERS

	Thermal channel	Visual channel
No. of channels	1	1-4
ADC	16-bit	16-bit
Resolution	300x280 analog input/interlace 256x256 digital/non-interlace	640(720)/480 interlace 640(720)/240 non-interlace
Memory buffer	1 MB	2 MB
DPLL clock recovery	yes	yes
Transfer rate	20MB/s - non burst 60MB/s - burst	20MB/s - non burst 60MB/s - burst
Real time capturing	yes	yes in low resolution
Supported cameras	Inframetrics® Series 600/700, AGEMA® Series 600/700/800 Hughes® TVS4000, FLIR SC1000	RS170, CCIR-PAL Radiological, ultrasound, visual cameras

II. 3D SCENE RECONSTRUCTION

3D image reconstruction is widely used in photogrammetry applications [3-5]. Up to now, 3D reconstruction was applied effectively for video images. It seems that combining video and thermal systems together with 3D image reconstruction procedures, provides new possibilities for thermography [3-4]. Localising an object in 3D space directly allows evaluating a distance and orientation of thermal specimen, and correct object's emissivity and ambient transmission for infrared radiation.

There are well known methods of 3-D image reconstruction. Methods called S*hape from Shading* and *Direct Linear Transformation* are the most exploited ones [1,4,5,6]. The numerical complexity and huge amount of information to be processed were the main obstacle for the practical implementation of 3D image reconstruction. New computer technology allows realising systems for such processing today [5].

S*hape from Shading* method assumes the illuminating the object from certain direction, and measuring the reflected radiation, which depends on the reflection angle (Fig. 2-3). This method is very sensitive to the color and non-homogeneity of the surface, as well as the illuminating radiation characteristics.

Report Documentation Page

Report Date	Report Type	Dates Covered (from... to)
25 Oct 2001	N/A	-

Title and Subtitle Computer System for Multispectral Image Acquasition and Processing	**Contract Number**
	Grant Number
	Program Element Number
Author(s)	**Project Number**
	Task Number
	Work Unit Number
Performing Organization Name(s) and Address(es) Institute of Electronics Technical University of Lodz Poland	**Performing Organization Report Number**
Sponsoring/Monitoring Agency Name(s) and Address(es) US Army Research, Development & Standardization Group (UK) PSC 802 Box 15 FPO AE 09499-1500	**Sponsor/Monitor's Acronym(s)**
	Sponsor/Monitor's Report Number(s)

Distribution/Availability Statement
Approved for public release, distribution unlimited

Supplementary Notes
Papers from 23rd Annual International Conference of the IEEE Engineering in Medicine and Biology Society, October 25-28, 2001, held in Istanbul, Turkey. See also ADM001351 for entire conference on cd-rom., The original document contains color images.

Abstract

Subject Terms

Report Classification unclassified	**Classification of this page** unclassified
Classification of Abstract unclassified	**Limitation of Abstract** UU

Number of Pages
4

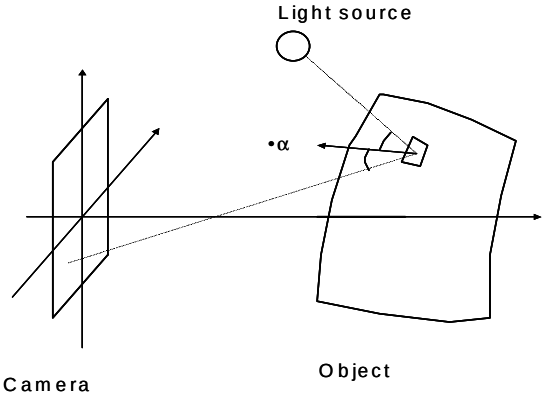

Fig. 2. "Shape from shading" method - principle

Fig. 3. "Shape from shading" method - results

The camera setup for 3D image reconstruction is shown Fig.4. We need to define 3D coordinates of 6 points for each image. These six reference are used for camera positioning. After positioning video cameras, any extra six points on both video and thermal pictures should be marked. These extra six points may be the same or different as reference ones used for video camera positioning. Program automatically calculates coordinates of this extra points and compute position of thermal camera without any given coordinates of marked points on thermal picture. This procedure is helpful when it is difficult to locate the details on the thermal image. On the other hand, in many practical cases it is possible to recognize the same points on each image, including the thermal one, without providing their real coordinates, what is also the 3D scene reconstruction algorithm. In the final stage of the algorithm, groups of three points marked by the user are used to determine the chosen planes for which, angle and distance are calculated, and used later for emissivity and temperature correction.

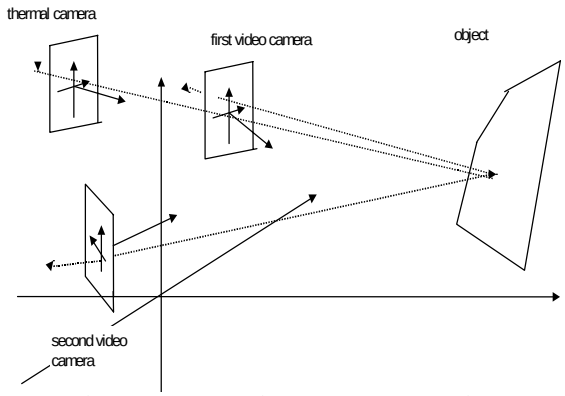

Fig. 4. Camera setup for 3D scene reconstruction

Each camera gives a different view of an observed object. Each 3D point visible on both pictures has its own (different for each one) 2D position. Differences between this locations on pictures obtained from different cameras are the base for computing the 3D position. The picture is a result of transformation of 3D object onto a flat surface of a CCD sensor in the camera. This transformation is afinic what makes possible to present the dependence between the coordinates of point in 3D space and in 2D picture.

Typically, two or more video cameras take pictures of the same object, so we can write set of such equation for each point and camera, and solve it to get 3D coordinates. Having more than 2 cameras, we can employ the least square algorithm to improve the measurement accuracy. The entire procedure is presented in *Fig. 5.*

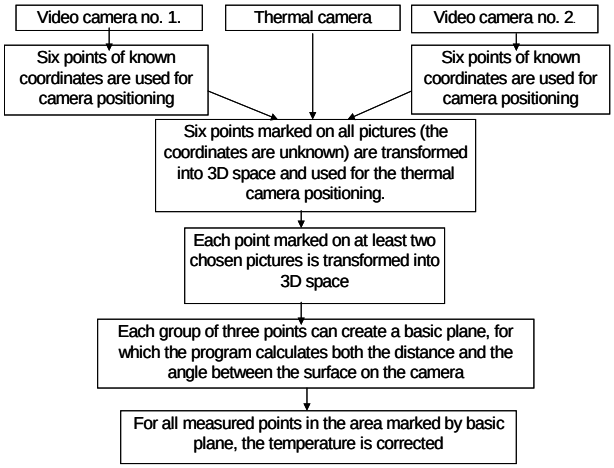

Fig. 5. DLT algorithm

The temperature measured by the thermal camera depends on the angles between the normal to this surface and the camera axis. The measured surfaced may be marked by three points, providing a surface's equation:

$$AX + BY + CZ + D = 0 \tag{1}$$

An angle η between camera's axis and the normal to the surface may be calculated from eqn.(1):

$$\cos\eta = \frac{\begin{bmatrix} A & B & C \end{bmatrix} \overline{m}^{-1} \begin{bmatrix} 0 & 0 & 1 \end{bmatrix}^T}{\left\| \begin{bmatrix} A & B & C \end{bmatrix} \right\|} \tag{2}$$

The real flux emitted by a piece of surface may be finally corrected using Lambert's law, as below.

$$\Phi = \frac{\Phi_0}{\cos\eta} \tag{3}$$

where: Φ_0, Φ denote the flux measured by the camera, and the one normal to the surface, respectively.

Results of temperature correction are presented in *Fig. 6* while the system for 3D reconstruction is in *Fig. 7.*

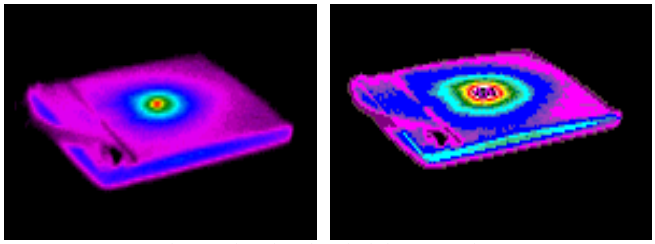

Fig. 6. Directional emissivity correction

Fig. 7. System for directional emissivity correction

II. PERSPECTIVE DISTORTION CORRECTION

In many practical cases an object is too close to the camera, or it can not be projected non perpendicular onto the detector plane. It is known as perspective distortion. In order to get the right view of the object, plane-to-plane transformation is used (*Fig. 8*). This method needs to use 4 reference points, as it has 8 transform parameters as shown in the eqn. (4).

$$\begin{cases} X_i = \dfrac{u_1 \cdot x_i' + u_2 \cdot y_i' + u_3}{u_7 \cdot x_i' + u_8 \cdot y_i' + 1} \\ Y_i = \dfrac{u_4 \cdot x_i' + u_5 \cdot y_i' + u_6}{u_7 \cdot x_i' + u_8 \cdot y_i' + 1} \end{cases} \quad (4)$$

where: u_i - transform coefficients; X,Y - co-ordinates after transformation (real co-ordinates); x',y'-co-ordinates of an original pixel.

The better results can be obtained using more reference points and applying the least-square approximation method. The results of 4-point projection are presented in *Fig.9*. The original image is a projection of a front building side on the plane not perpendicular to the camera optical axis. The windows shown there are not of the rectangular shape. After transformation of the front building plane, on the plane normal to the camera axis, the windows become rectangular. The entire scene keeps the real aspect ratio significantly reducing the perspective distortions. After such correction it is quite easy to stick together a set of images and present the whole scene in the orthogonal projection [1,5].

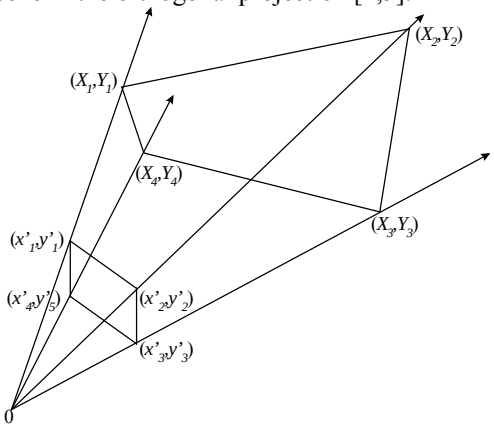

Fig. 8. Perspective distortion correction, plane-to-plane transformation

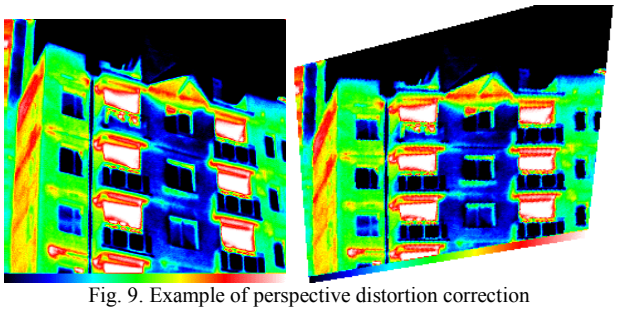

Fig. 9. Example of perspective distortion correction

Another tool makes possible to overlay visual and thermal images. The assumption of such superimposing is that the thermal and visual images are projected on the same or parallel planes. We can easily wrap, shift and mix two images. It simplifies or in certain cases allows locating precisely the hot spots. Two images (thermal and optical) allow (by using common cursor) indicating a certain point on CCD scene, and read temperature on thermal one.

III. SPECTRAL EMISSIVITY

Emissivity was introduced to characterize the optical properties of materials in sense of amount of enegry emitted in comparison with ideal black body. Radiation of black body is described by emissive power $e_b(\lambda,\varphi,\theta)$ related to power emitted from unit elemental surface, into unit elemental solid angle in $d\lambda$ spectral range (*Fig. 10*). Unlike the emission, the radiation intensity $i_b(\lambda)$ is defined on the basis of projected area [1,2] and it *does* not depend on direction, (*Fig. 10*). Total monochrome emission power passing hemisphere takes a form:

$$e_{b,\lambda} = i_b(\lambda) \int_{\varphi=0}^{2\pi} \int_{\theta=0}^{\frac{\pi}{2}} \cos(\varphi)\sin(\varphi) d\theta d\varphi = \pi i_b(\lambda) \quad (5)$$

Total radiation intensity can be evaluated using Planck law as:

$$I_b = \int_0^{\infty} i_b(\lambda) d\lambda = \frac{\sigma}{\pi} T^4 \quad (6)$$

while the total emission power: $E_b = \sigma T^4$

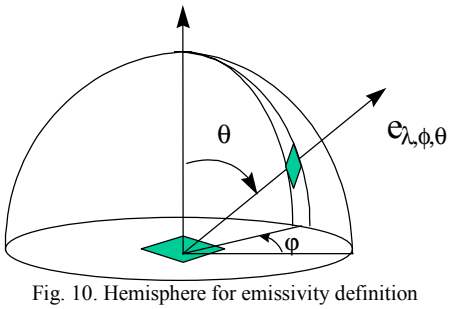

Fig. 10. Hemisphere for emissivity definition

Based on total, monochrome and directional quantities representing the amount of energy emitted we can define the following emissivities.

Directional monochromatic emissivity

$$\varepsilon_{\lambda,\theta,\varphi} = \frac{e_{\lambda,\theta,\varphi}}{e_{b,\lambda,\theta,\varphi}} = \frac{e_{\lambda,\theta,\varphi}}{e_{b,\lambda,n}\cos\varphi} \quad (7)$$

Monochromatic normal emissivity

$$\varepsilon_{\lambda,n} = \frac{e_{n,\lambda}}{e_{b,\lambda,n}} \tag{8}$$

Directional total emissivity

$$\varepsilon_{\theta} = \frac{E_{\theta,\varphi}}{E_{b,\theta,\varphi}} = \frac{\pi \int_0^{\infty} e(\lambda,\theta,\varphi)d\lambda}{\sigma T^4 \cos\theta} \tag{9}$$

Hemispherical total emissivity

$$\varepsilon = \frac{E}{E_b} = \frac{\int_0^{\infty} \varepsilon_{\lambda} e_{b,\lambda} d\lambda}{\sigma T^4} \tag{10}$$

where ε_λ is the hemispherical spectral emissivity defined as:

$$\varepsilon_{\lambda} = \int_0^{2\pi} \int_0^{\frac{\pi}{2}} \varepsilon_{\lambda,\varphi,\theta} d\theta d\varphi \tag{11}$$

Having so many different quantities defining emission properties of the real body it seems to be quite difficult to evaluate the emissivity in practice [2,6].

There are some methods for emissivity evaluation. One of the first method of emissivity equalising was based on covering surface by thin layer with high and known emissivity factor. Typically, one can use black paint with the emissivity factor ε=0.95-1 to cover measured object. This simple method has basic limit of its application – covering even by very thin layer changes slightly the heat transfer in the investigated body and in some practical cases it is simple impossible, e.g. because of high voltage.

The other approach to emissivity evaluation is based on calorimetic surveys. So far we know the object temperature and the radiation level by thermographic measurement, the simple formulas give the emissivity factor estimation [6].

Using the system described above we can evaluate spectral emissivity for opaque materials by measuring the its reflectivity, as expressed below:

$$\varepsilon_{n,\lambda} = 1 - \rho_{n,\lambda} \tag{12}$$

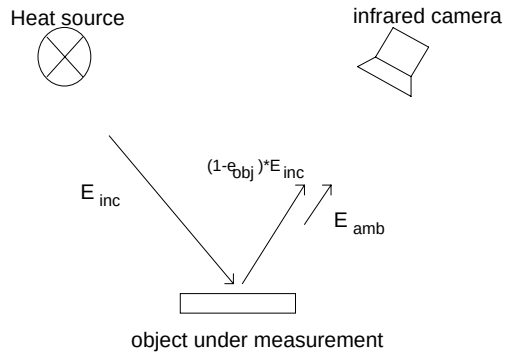

Fig. 11. Evaluation of emissivity by reflection

In order to evaluate the emissivity by reflection, two measurements must be performed. First one is to calibrate the system by measuring the heat source energy. It is done by reflection from the infrared mirror, e.g.: from the polished cooper. The energy is expressed by temperature of the heat source T_{Cu}. Then, the radiation energy reflected by the investigated sample is measured T_m (*Fig. 11*). Including the ambient temperature, and assuming the very high reflectance of the mirror, we can obtain the unknown emissive factor.

$$\varepsilon = 1 - \frac{T_m^4 - T_{amb}^4}{T_{Cu}^4 - T_{amb}^4} \tag{13}$$

Some thermal cameras are equipped with broadband (BB) detectors, such as microbolometers or BB photon ones. By using build in the camera band pass filters differentiating short-wavelength (2-5μm) with long-wavelength (8-12 μm), it is possible to evaluate the emmisivity for both spectral ranges. Having the emissivity maps for investigated surfaces, it is easy to correct the temperature measured the thermographic camera [6].

IV. CONCLUSION

The system for thermal and visual image processing is presented in this work. This system can be used for capturing images in real-time, frame-by-frame, or storing the sequence with defined interval between the following images. It is actually used for advanced thermal and visual images processing, e.g. 3-D photogrametry reconstruction, noise cancelling, image superimposing, etc., and improves the thermal camera measuring parameters.

The methods presented in this paper give the ability to reconstruct 3D coordinates of measured object, including the positions of all cameras used for the measurements. It allows computing both the angles between camera's axes and normal to the measured surface and the distance between the camera and the object. This is necessary for the correction of emissivity, and in consequence the temperature measured by camera. Although the methods presented in this paper are based on well-known algorithms, a few new improvements were added to include thermal system for photogrammetric application.

REFERENCES

[1] W. K. Pratt, "Digital Image Processing", Willey & Sons, Inc, Ney York, 1991.

[2] R. Siegel, J. Howell: „Thermal radiation heat transfer". New York, Hemisphere Publishing Corp, 1989, ISBN 0-89116-506-1.

[3] B. Więcek, S. Zwolenik, P. Sawicki, "Advanced Multichannel Thermal and Visual System", III International Workshop Advances in Signal Processing for NDE of Materials, The American Society for Nondestructive Testing, Inc., Columbus Ohio, 1998, 289-294.

[4] B. Więcek, P. Sawicki, R. Stein, "3-D reconstruction for video and thermal images", 4th International Workshop Advanced Infrared Technology and Applications, Florence'97, Florence, Sept. 15-16, 1997.

[5] P. Sawicki, B. Więcek, "CCD Multicameras interactive digital system for close range photogrammetric applications", International archives of photogrametry and remote sensing, Vienna, Austria, 1996.

[6] B. Więcek, P. Sawicki, R. Stein, "Directional Emissivity Correction in Thermal and Visual Systems", III International Workshop, Advances in Signal Processing for NDE of Materials, The American Society for Nondestructive Testing, Inc., Columbus Ohio, 1998, 351-356.